

Kinetic Study for Reactive Red 84 Photo Degradation Using Iron (III) Oxide Nanoparticles in annular reactor

Cano-Guzmán CF^{1*}, Pérez-Orozco JP², Hernández-Pérez I³, González-Reyes L³, Garibay-Febles V⁴ and Suárez-Parra R¹

¹Instituto de Energías Renovables IER-UNAM, Priv. Xochicalco S/N, Temixco, Morelos 62580 México

²Instituto Tecnológico de Zacatepec, Departamento de Ingeniería Química y Bioquímica, Calzada Tecnológico No. 27, Col. Centro, Zacatepec, Morelos, México

³Universidad Autónoma Metropolitana-A, Dpto. de Ciencias Básicas, Av. Sn. Pablo No. 180, México, D.F. 02200, México

⁴Instituto Mexicano del Petróleo, Laboratorio de Microscopía de Ultra Alta resolución, Eje Central Lázaro Cárdenas Norte 152 Colonia San Bartolo Atepehuacan, 07730, México

Abstract

Iron oxide nanoparticles (Fe₂O₃ NPs) were prepared by mixing iron(II) sulfate (FeSO₄) and hydrogen peroxide (H₂O₂) in aqueous solution at pH 3. Fe₂O₃ NPs are used to degrade Reactive Red-84 (RR-84) azo dye in a glass annular photo-reactor using a white light lamp. The presence of Fe₂O₃ NPs was verified by HRTEM analyses. Kinetic studies were made varying the reagents concentration and the reaction rate was controlled increasing the concentration of iron ions in comparison with H₂O₂. Langmuir-Hinshelwood (L-H) kinetic model was performed to analyze heterogeneous catalytic reactions under illumination conditions. The elimination process of azo dye followed the pseudo first-order kinetic according to L-H model. The adsorption process of the azo dye on the catalytic surface was determinant for the dye photodecomposition. The linear expression of the Langmuir adsorption isotherm under darkness was further used to establish the maximum amount of dye adsorbed $Q_{max} = 0.80 \pm 0.18 \text{ mg} \cdot \text{mg}_{catalyst}^{-1}$ and the adsorption constant $k_{ads} = 0.016 \pm 0.004 \text{ L} \cdot \text{mg}^{-1}$. The Langmuir-Hinshelwood equilibrium constant for dye adsorption under illumination conditions was $K_{L-H} = 0.03 \pm 0.02 \text{ L} \cdot \text{mg}^{-1}$. This similarity with adsorption constants could depict an evidence which suggest that Fe₂O₃ NPs are presents in Fenton's reaction (FeSO₄/H₂O₂) interacting as catalysts in the degradation of organic substrates.

Keywords: Photo-degradation; Azodye; Iron oxide nanoparticles (Fe₂O₃ NPs); Adsorption

Introduction

Nowadays, water pollution reaches rivers, lakes, ravines and oceans, representing a serious problem for environment. The significant reduction of fresh water demands that the treatment systems of polluted waters must be optimized to re-use wastewater at least in irrigation, of agricultural areas. The wastewaters from industrial textile processing contain dyes in different concentrations and usually they are sent to sewage treatment plants, which use conventional degradation systems of organic pollutants such as aeration with activated sludge, also called microbiological treatments. However, these systems cannot degrade recalcitrant compounds as azo dyes [1]. In addition, these pollutants will always be present in marine ecosystems with a very low concentration, dangerously polluting the marine environment. For this reason, a feasible solution would be to treat the polluted water inside the textile factories using photocatalytic reactors, eliminating the azo dyes or at least, breaking the molecules of these compounds and stimulating the formation of other less hazardous organic compounds that can be eliminated with microbiological treatments [2].

The Advanced Oxidation Processes (AOP) of organic compounds employ heterogeneous photocatalytic reactions with semiconductor materials usually known as photocatalysts and an oxidant agent as ozone (O₃), hydrogen peroxide (H₂O₂) or oxygen (O₂). The most used photocatalysts to degrade organic compounds in aqueous suspensions are TiO₂ and ZnO [3]. Also, the organic pollutants can be eliminated by a Fenton's reaction, using iron salts in aqueous solution (FeCl₂, FeCl₃, FeSO₄ and Fe₂(SO₄)₃ and H₂O₂ as oxidant agent at acid conditions, pH (2-3) [4,5]. Fenton's reaction was proposed in 1894 and establishes that it is a homogeneous system based in redox processes of iron ions, which reduce H₂O₂ molecules forming *OH radicals that are considered very active species to destabilize the molecular structure of organic compounds [6-8]. Some researchers found that the iron ions

Fe²⁺ from the iron precursor salts are more active than Fe³⁺ due to the lack of reducing power of iron(III) ions [5]. However, Suárez-Parra et al. [9] found that at pH 3.8, Fe₂O₃ NPs prepared with FeCl₃ as iron precursor salt are more active than Fe₂O₃ NPs prepared with FeCl₂ to degrade phenol, 2-chlorophenol and o-cresol, using H₂O₂ as oxidizing agent under similar conditions to Fenton's reaction but at higher pH (3.8). Furthermore, these authors detected and identified by TEM and XRD, the presence of different Fe₂O₃ phases (α -Fe₂O₃, β -Fe₂O₃, γ -Fe₂O₃, ϵ -Fe₂O₃, FeO(OH), β -FeOOH) in an aqueous colloidal system prepared with FeCl₂/H₂O₂ or FeCl₃/H₂O₂. The photodecomposition of phenol and its derivatives was attributed to one of these Fe₂O₃ phases that could act as photocatalyst or as Lewis acid catalyst and both systems take into account the presence of particles that could carry out adsorption systems.

Langmuir-Hinshelwood (L-H) pseudo first order model has been employed to analyze photocatalytic oxidation kinetics of many organic compounds on heterogeneous catalysts, evaluating the adsorption of organic azo dyes on surface catalytic sites of some solid materials [10-13]. The model determines the relationship between the initial degradation rate and the initial concentration of the organic adsorbate

***Corresponding author:** Cano-Guzmán CF, Instituto de Energías Renovables, Universidad Nacional Autónoma de México, Priv. Xochicalco s/n, Temixco, Morelos 62580, Mexico, Tel: +52-55-56-22-98-20, Fax: +52-5-5-2-9-42; E-mail: cfcg@ier.unam.mx

Received January 15, 2014; **Accepted** February 07, 2014; **Published** February 09, 2014

Citation: Cano-Guzmán CF, Pérez-Orozco JP, Hernández-Pérez I, González-Reyes L, Garibay-Febles V, et al. (2014) Kinetic Study for Reactive Red 84 Photo Degradation Using Iron (III) Oxide Nanoparticles in annular reactor. J Textile Sci Eng 4: 155. doi:10.4172/2165-8064.1000155

Copyright: © 2014 Cano-Guzmán CF, et al. This is an open-access article distributed under the terms of the Creative Commons Attribution License, which permits unrestricted use, distribution, and reproduction in any medium, provided the original author and source are credited.

expressed by eq. 1 [10-12]:

$$\frac{1}{k_{obs}} = \frac{1}{K_{L-H}k} + \frac{[RR-84]_0}{k} \quad (1)$$

Where $[RR-84]_0$ is the initial concentration ($\text{mg}\cdot\text{L}^{-1}$) of the organic azo dye, K_{L-H} is the Langmuir-Hinshelwood (L-H) adsorption equilibrium constant ($\text{L}\cdot\text{mg}^{-1}$) and k is the reaction rate constant on catalyst surface ($\text{mg}\cdot\text{L}^{-1}\cdot\text{min}^{-1}$). This L-H reaction kinetic model has been successfully related with experimental data in AOP of just a single organic compound [10-12].

In order to describe the reaction behavior, some authors have proposed several models and one of the most common is the L-H type. The photocatalytic degradation of RR-84 under illumination conditions can be followed considering the concentration changes and the following equation can be employed:

$$r_{\phi} = \frac{kK_{L-H}[RR-84]_0[H_2O_2]_0\phi S_i}{(1+K_{L-H}[RR-84]_0)} \quad (2)$$

Where k , K_{L-H} , $[RR-84]_0$ are the same parameters mentioned previously, $[H_2O_2]_0$ is the initial H_2O_2 concentration, ϕ is the photonic flux and S_i are the illuminated catalytic active sites.

Besides, it is necessary to measure the adsorption process under darkness in order to verify and compare with L-H models under illumination conditions. The K_{L-H} obtained must be similar to that obtained in equilibrium dark adsorption analysis for L-H model can be validated [12]. However, in other studies the adsorption constants under illumination or darkness conditions have been reported with substantially different values [15,16].

In this work, Fe_2O_3 NPs were prepared by the interaction of $FeSO_4/H_2O_2$ at pH 3 to degrade RR-84 azo dye using $100 \text{ mg}\cdot\text{L}^{-1}$ as initial concentration in a glass annular photo-reactor, utilizing 2.5 L of reaction mixture and a 8 W visible light lamp. The Fe_2O_3 NPs presence was observed by HRTEM and a couple of Fe_2O_3 phases were found. A kinetic study was performed increasing the iron quantity in the iron precursor salt and maintaining H_2O_2 concentration constant and vice versa. In order to validate the presence of a heterogeneous catalyst (Fe_2O_3 NPs) in an apparently homogeneous reaction (Fenton's process $FeSO_4/H_2O_2$ at pH 3), it was performed an evaluation of adsorption constants for RR-84 azo dye obtained under darkness and illumination conditions using a 8W visible light lamp by means of Langmuir isotherms.

Materials and Methods

Chemical reagents

The iron salt $FeSO_4$ (99.9%) and hydrogen peroxide (H_2O_2 30%) were obtained from FERROMONT and used without further purification. The pure dye RR-84 $C_{26}H_{19}BrN_4Na_2O_9S_3$ (C.I. No. 13429, CAS No. 85187-33-3/61969-27-5, MW=753.53) was acquired from Rintex Textile company. In Figure 1 is shown the molecular structure of RR-84. Only deionized water was employed in this study avoiding any kind of interferences.

Preparation of the iron (III) oxide (Fe_2O_3) catalyst.

In order to degrade the azo-dye, the initial iron concentration in the $FeSO_4$ salt was $5.584 \text{ mg}\cdot\text{L}^{-1}$ and the H_2O_2 initial concentration was $1200 \text{ mg}\cdot\text{L}^{-1}$ for the kinetic studies. In each experiment, using a beaker

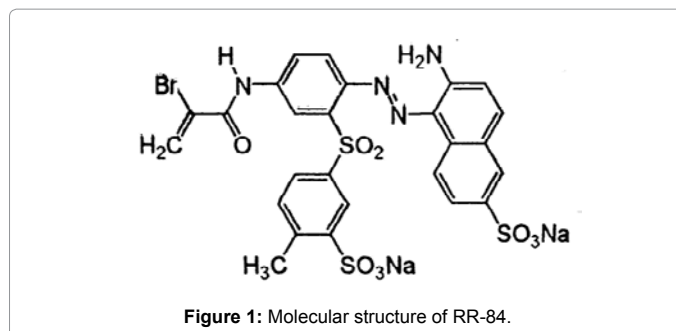


Figure 1: Molecular structure of RR-84.

of 4L, 250 mL of iron salt solution ($C_{Fe^{+2}}=55.84 \text{ mg}\cdot\text{L}^{-1}$) was diluted in 1 L of deionized water and mixed with the solution of 10 mL of H_2O_2 (30%) previously diluted in 1.115 L of deionized water; in all cases the solution of H_2O_2 was slowly added to the iron salt solution expecting the formation of Fe_2O_3 NPs at pH 3.5. Immediately, the pH was adjusted to 3 using some drops of 0.1 M sulfuric acid solution. Finally, to start the photo catalytic reaction it was added 125 mL of azodye RR-84 ($2000 \text{ mg}\cdot\text{L}^{-1}$) achieving an initial concentration of $100 \text{ mg}\cdot\text{L}^{-1}$ in the reaction mixture for the kinetic studies varying the reagents concentration. The final volume of the reaction mixture was 2.5 L.

Catalyst characterization

The aqueous mixture of $FeSO_4/H_2O_2$ at pH 3 was analyzed by HRTEM, in order to detect the presence of Fe_2O_3 NPs and measure their size, trying to identify the iron oxide phase(s) that could be present in the suspension. Some droops of this suspension were placed on a copper grid to be analyzed on a High Resolution Transmission Electron Microscopy, Tecnai G2 F30 microscope, operated at 300 kV with a point resolution of 0.2 nm and $C_s=1.2 \text{ nm}$.

Reaction system

In order to determine the catalytic activity of Fe_2O_3 NPs, RR-84 azodye was selected as pollutant due to its recalcitrant stability. The RR-84 concentration was followed with the calibration curve using the next concentrations: 100, 80, 60, 40, 20 and $2 \text{ mg}\cdot\text{L}^{-1}$, each concentration corresponds to an absorbance value. To obtain dye concentration, the samples were taken of the reaction mixture in different times (0, 5, 10, 20, 40, 80, 120 and 180 minutes) and the absorbance values were measured following the wavelength signal in 497 nm with a spectrophotometer UV-Vis HACH (DR 5000) using quartz cells with 1 cm light path. The reaction system consists of a peristaltic pump with variable volumetric flow. The recirculation of the reaction mixture was performed with clearplastic hoses linking the annular reactor with a storage tank. Assuming that there is no RR-84 photodegradation reaction in the hoses, the reaction mixture inside the storage tank was in constant stirring to keep a homogeneous concentration of RR-84. A 8W visible light lamp TECNO LITE (F8T5D) was located inside the reactor without touching the reaction mixture, simulating sunlight. The experimental annular photocatalytic reactor is shown in the Figure 2. The sample was taken to the output of return hose in the storage tank.

Equilibrium adsorption measurements under dark conditions

0.5 L of reaction mixture $FeSO_4/H_2O_2$ prepared as mentioned above in section 2.2 was aged by three months expecting the maximum production of Fe_2O_3 NPs and the inactivity of $\cdot OH$ radicals formed by the reduction of H_2O_2 molecules. In a 250 mL amber Erlenmeyer flask, the samples were mixed with different azodye initial concentrations ($100, 80, 60, 40$ and $20 \text{ mg}\cdot\text{L}^{-1}$) and the corresponding amount of the

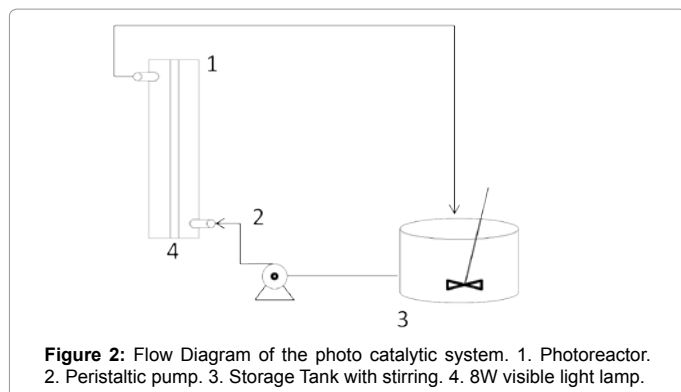


Figure 2: Flow Diagram of the photo catalytic system. 1. Photoreactor. 2. Peristaltic pump. 3. Storage Tank with stirring. 4. 8W visible light lamp.

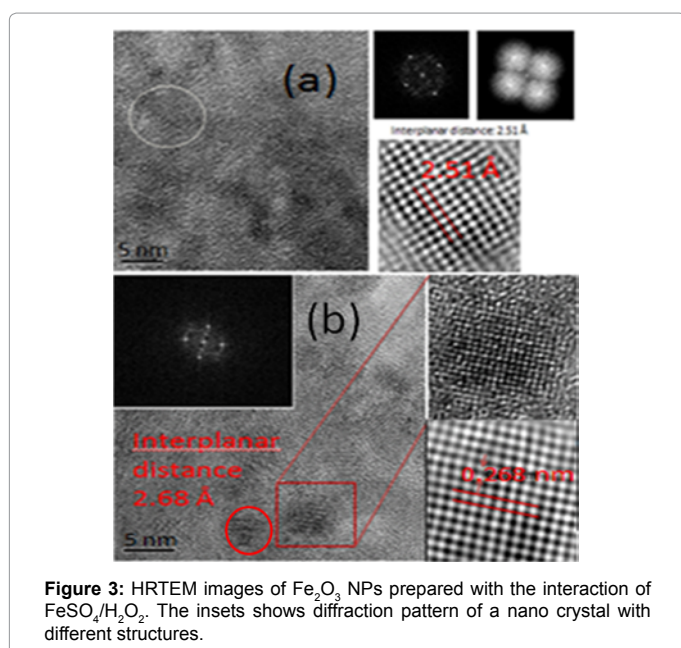


Figure 3: HRTEM images of Fe_2O_3 NPs prepared with the interaction of $\text{FeSO}_4/\text{H}_2\text{O}_2$. The insets show diffraction pattern of a nano crystal with different structures.

reaction mixture. The final volume in these suspensions was 0.1 L. The flasks were covered with black bags from the beginning. The samples in the flask were stirred only during the first 20 minutes, expecting the sedimentation Fe_2O_3 NPs after this time and were maintained without stirring until 16 hours. The samples for the measurement of UV-Vis absorbance in the spectrophotometer were taken from the liquid surface in the reaction mixture. The RR-84 absorbance was followed each hour until this value was kept constant. The last reading of absorbance (at 16th hour) was considered as the equilibrium concentration employing these azodyes dilutions as calibration curves specifically for this study.

Results and Discussion

The photocatalytic reaction takes place on Fe_2O_3 semiconductor surface as follows: the photocatalyst is irradiated with visible light in the wavelength range of 380–750 nm, this radiation is capable of producing electron-hole pairs in its surface, the electrons are aligned on conduction band favoring the reduction of H_2O_2 molecules into $^*\text{OH}$ radicals [10], which are very active species to destabilize the azo dye molecules. On the other hand, holes are present in the valence band, ready to adsorb the azo dye molecules on its surface, attaching them in the holes and increasing the probability that $^*\text{OH}$ radicals interact chemically with azo dye molecules, destabilizing mainly the double bonds in their chemical

structure. Besides of this photocatalytic behavior, if the Fe_2O_3 NPs act as Lewis acid catalysts, which were mentioned in a previous study [9], the antibonding orbital in the molecules of Fe_2O_3 is freestimulating the adsorption of any azo dye chemical bond able to share an electron pair. The strong interaction between Fe_2O_3 with electron pair destabilizes the binding of azo dye and breaks in the absence of light mainly.

Results of the characterization of Fe_2O_3

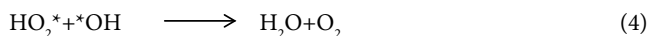
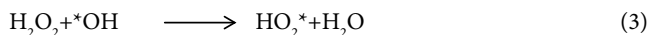
In Figure 3, it can be seen two images of the HRTEM analysis for Fe_2O_3 NPs obtained. In the Figure 3a on the left side it is observed the formation of crystals with different morphologies and at the bottom right side there is an analysis of the inter-planar distances (2.51 Å), taking into account the circumference area marked on the left side, that can be compared with a diffraction pattern and confirms the presence of one iron oxide phase. This inter-planar distance, which is related with maghemite iron oxide phase ($\gamma\text{-Fe}_2\text{O}_3$) was compared with the card JCPDS 00-039-1346 corresponding to the plane (311). In the Figure 3b, on the bottom left side is observed the formation of crystals with different morphologies and sizes from 3 to 5 nm (circle and square, respectively), the image on the upper right side corresponds to: an amplification of nanoparticle (within the selected square area), the diffraction pattern of all nanoparticles found and the roughness of the nano-crystal in the selected area. The presence of bright spots (and diffuse rings) in the diffraction pattern is associated with the formation of nano-crystals within the aqueous suspension of Fe_2O_3 sample. Besides, this same figure shows an arrangement with an inter-planar distance of 2.68 Å that could be fitted with hematite iron oxide phase ($\gamma\text{-Fe}_2\text{O}_3$) corresponding to the plane (104) according to the card JCPDS 00-001-1053. Furthermore, the dark images in both figures correspond to the comparison between the structure and the simulation of Fast Fourier Transform (FFT). It is also important to highlight the presence of structural defects (point and surface) on the surface of the nanoparticles, which could contribute to the increase of specific area and the photocatalytic activity.

These analyses confirmed the presence of two iron oxide phases in an aqueous suspension in the reaction mixture $\text{FeSO}_4/\text{H}_2\text{O}_2/\text{H}_2\text{O}$ at pH 3. And this result could be considered as evidence that there are different iron oxide phase(s) in this known Fenton's reaction. At this point, is feasible to think that one of these phases could behave as photocatalyst and another could be acting as Lewis acid catalyst since the photocatalytic oxidation of RR-84 is performed in a shorter time of reaction under illumination as well as under darkness but with a lower photodegradation rate (results not shown). The Fe_2O_3 NPs activity even under darkness could be explained by Lewis acid catalyst behavior and its interaction as photocatalyst or as Lewis acid catalyst could be related with a phase(s) relationship.

Kinetic study of the RR-84 photodegradation using reagent concentration variations

The initial concentration of RR-84 for these kinetic studies and for effect of catalyst concentration was fixed in $100 \text{ mg}\cdot\text{L}^{-1}$. The catalyst (Fe_2O_3 NPs) concentration cannot be determined due to the nano structure of the particle size; however we used the iron concentration from the iron precursor salt to express the mass of the catalyst. The initial concentration of iron in 2.5 L of reaction mixture was $5.584 \text{ mg}\cdot\text{L}^{-1}$ or 0.0139 g of iron expressed in mass. The iron concentration was increased from its initial value for these kinetic studies maintaining the H_2O_2 concentration constant. The Table 1 demonstrates the dependence of the RR-84 photodegradation rate on iron concentration to form Fe_2O_3 NPs that interact as photo catalysts. In this Table it

was observed that an increase in the iron concentration leads to an improvement in the RR-84 photodegradation rate due to an increase of the catalytic active sites. Indeed, a higher concentration of catalyst increases its interaction with the visible radiation and consequently, there is a higher contact with H₂O₂ to form *OH radicals on Fe₂O₃ NPs surface. On the other hand, azo dye molecules adsorbed on the surface of the Fe₂O₃ NPs raise the probability to meet *OH radicals and this interaction could destabilize RR-84 at higher reaction rates. However, this increase in iron concentration shows a limit in its activity as can be seen in the Figure 4. In the Table 2, the initial concentration of H₂O₂ employed was 1200 mg*L⁻¹, representing an excessive quantity with respect to iron concentration. The H₂O₂ amount was duplicated (2400 mg*L⁻¹), triplicated (3600 mg*L⁻¹) and quadrupled (4800 mg*L⁻¹) analyzing the photodegradation rate of RR-84 and kinetic studies were performed keeping constant iron concentration. The increase of oxidizing agent also reflects an improvement in the photodegradation rate, probably due to a raised in the generation of *OH radicals present in the reaction mixture [16] that helps to destabilize the molecular structure of dye at higher rates. However, high dosage of oxidizing agent (H₂O₂) is a powerful *OH scavenger [17,18] as next equations show:



Hachem [17] reported that there is a competition for adsorption on the TiO₂ catalytic sites between the azo dyes and H₂O₂ molecules at pH 5. Thus, high concentrations of H₂O₂ could stimulate the adsorption of this substrate on the Fe₂O₃ NPs catalytic active sites and could affect the RR-84 degradation rate. This behavior could explain the limit in the catalytic activity due to the increase in the H₂O₂ concentration as is

| [Fe]/[H ₂ O ₂] (mg/L) | k _{obs} (min ⁻¹) | R ² |
|--|---------------------------------------|----------------|
| [5.584]/[1200] | 0.008 ± 0.0001 | 0.9854 |
| [11.168]/[1200] | 0.0154 ± 0.00045 | 0.9737 |
| [16.752]/[1200] | 0.021 ± 0.0015 | 0.9563 |
| [22.336]/[1200] | 0.023 ± 0.0021 | 0.9515 |

Table 1: Apparent pseudo first order rate constant varying the concentration of iron to form Fe₂O₃ NPs in the degradation of RR-84.

| [Fe]/[H ₂ O ₂] (mg/L) | k _{obs} (min ⁻¹) | R ² |
|--|---------------------------------------|----------------|
| [5.584]/[1200] | 0.008 ± 0.0001 | 0.9854 |
| [5.584]/[2400] | 0.0192 ± 0.0013 | 0.9852 |
| [5.584]/[3600] | 0.0204 ± 0.0015 | 0.985 |
| [5.584]/[4800] | 0.0213 ± 0.0015 | 0.9877 |

Table 2: Apparent pseudo first order rate constant varying the concentration of hydrogen peroxide to form Fe₂O₃ NPs in the degradation of RR-84.

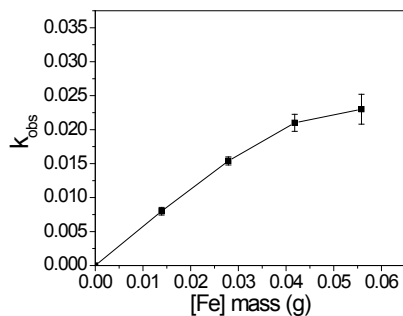


Figure 4: Effect of [Fe] mass to produce Fe₂O₃ NPs on the apparent rate constant (k_{obs}) during the photo catalytic reactions.

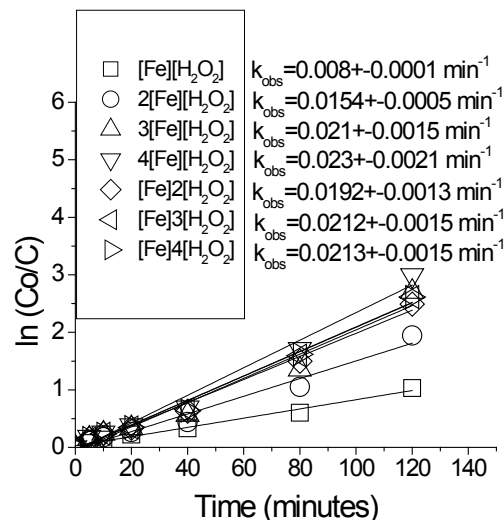


Figure 5: Linear variation of ln(Co/C) as a function of time for the photocatalytic discoloration of RR-84 changing the reactant concentrations.

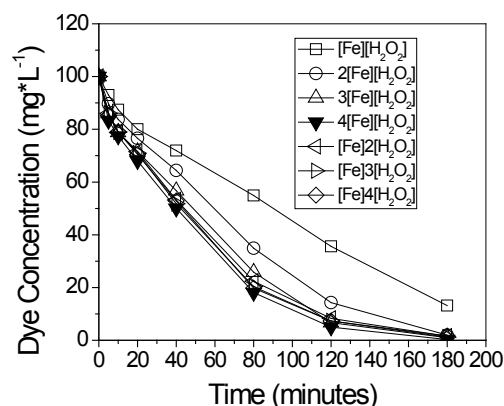


Figure 6: Changes in the photocatalytic discoloration of RR-84 versus time varying the concentration of reactants.

shown in the Table 2, analyzing the k_{obs} values.

The apparent pseudo first order constants were evaluated plotting the natural logarithm of Co/C as a function of time using the first order kinetic analysis, expressed by the eq. 5 and are depicted in the Figure 5, using the dye concentration data of the discoloration curves shown in the Figure 6. The Table 1 shows that the RR-84 photocatalytic reaction rate is controlled by the iron concentration, due to it is the limiting reactant in the process and an increase in its concentration stimulate the formation of a greater amount of Fe₂O₃ NPs. In the Table 2, similar results are obtained with high concentration of H₂O₂ (4 times more than originally) in comparison with iron concentration. However, in this case, the reaction rate increasing the H₂O₂ concentration cannot exceed the reaction rate with iron concentration increased fourfold, this behavior may indicate that the reaction could be performed decreasing H₂O₂ concentration in the original reaction, exhibiting high reaction rates and reducing processing costs.

Effect of catalyst concentration

Analyze the effect of catalyst concentration is fundamental to follow

RR-84 photodiscoloration rate in slurry photocatalytic processes. Parra [18] mentioned that the mass of catalyst required is a function of the dye concentration and the geometry of the reactor. The Figure 6 shows the apparent rate constant (k_{obs}) as a function of iron amount used, the initial concentration of H_2O_2 to degrade RR-84 ($1200 \text{ mg}\cdot\text{L}^{-1}$) was kept constant. At the beginning, the Increase of iron quantity above 0.014 g leads to an increase in the photocatalytic reaction rate. However, there is a point where an increase in the iron concentration does not affect the photocatalytic reaction rate reaching a limit in the photodegradation. This behavior confirms that if the catalyst mass is increased, there will be a greater amount of surface active sites and this effect is improved with nanostructure materials as in the case of Fe_2O_3 NPs.

The limit in the reaction rate with respect to $[Fe]$ mass in grams, also could be explained due to a greater quantity of Fe_2O_3 NPs present in the reaction mixture, this agglomeration of NPs could block the radiation of the incident light in some NPs inside the reactor, how has been proposed by other authors [11], and this leads to a decreasing in the photocatalytic activity.

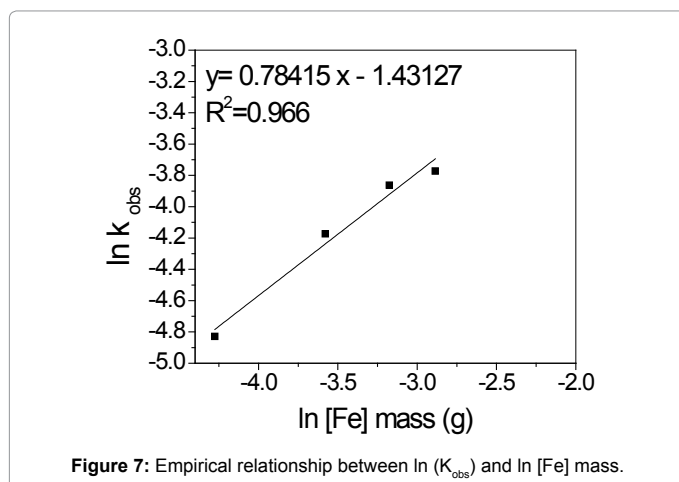
To analyze the reaction kinetics using dyes, Galindo [19] proposed an empirical relationship between the initial discoloration rate and the heterogeneous catalyst mass ($r_0[\text{catalyst}]^n[\text{dye}]$), being "n" an exponent less than 1 for all dyes studied that represents the slope of the straight line directly in a graphic of K_{obs} versus catalyst mass [17,20], taking into account low concentrations of catalyst.

In the Figure 7 is plotted the natural logarithm of RR-84 apparent rate constant as a function of the natural logarithm of the catalyst mass and the dependence of the $[Fe]$ mass to form Fe_2O_3 NPs on the initial discoloration rate (r_0) of RR-84 follows a similar relationship to ($r_0 \propto [Fe_2O_3]^{0.78 \pm 0.06}$). This result suggests that the system could be related with the degradation of a dye using a solid catalyst.

Photocatalytic degradation kinetics

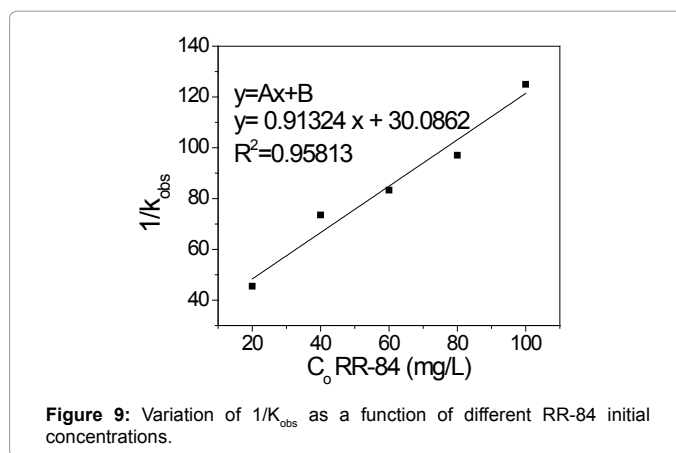
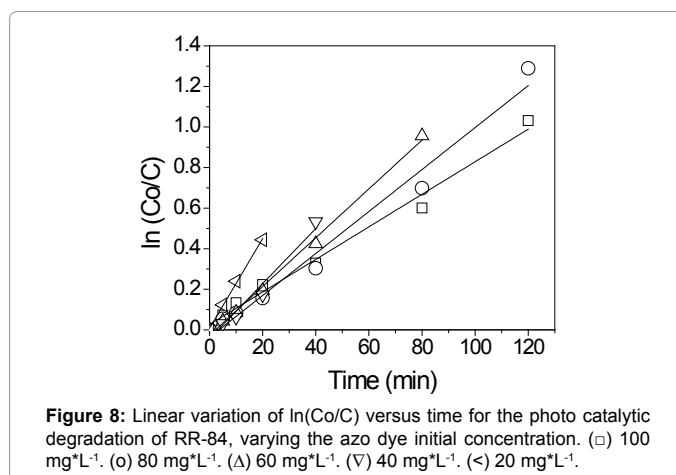
In the Table 3 can be seen that the kinetic rate constant decrease with the increase of the dye initial concentration. Many authors have proved that among fewer dye initial concentration exist, the kinetic rate constant is increased [12,20]. The RR-84 degradation experiments with visible light in aqueous suspensions, employing Fe_2O_3 NPs followed a kinetic of pseudo-first-order with respect to the dye concentration in the reaction mixture:

$$r = -\frac{dC}{dt} = k_{obs}C \quad (5)$$



| Co ($\text{mg}\cdot\text{L}^{-1}$) | K_{obs} (min^{-1}) | R^2 |
|--------------------------------------|---------------------------------|--------|
| 20 | 0.022 ± 0.0061 | 0.9968 |
| 40 | 0.0134 ± 0.0017 | 0.9996 |
| 60 | 0.012 ± 0.0007 | 0.9951 |
| 80 | 0.0103 ± 0.0003 | 0.9778 |
| 100 | 0.008 ± 0.0001 | 0.9854 |

Table 3: Pseudo first order apparent rate constant values for the different initial concentrations of RR-84.



The integration of eq. (5) (between the limits C_0 at $t=0$, and C at $t=t$, being C_0 the initial concentration of dye in the reaction mixture and C the dye concentration at the reaction time $t=t$) will lead to the next equation:

$$\ln\left(\frac{C_0}{C}\right) = k_{obs}t \quad (6)$$

Where k_{obs} is the apparent pseudo-first-order rate constant and the variation of the dye concentration influences directly to this constant. The Figure 8 shows $\ln(C_0/C)$ as a function of reaction time, varying the initial concentration of RR-84.

The k_{obs} values are obtained from the slope in the linear regression analysis of the concentration curves, in a similar form how were obtained in the Figures 5 and 6. The Table 3 shows the k_{obs} values of different RR-84 initial concentrations and their regression coefficients.

The L-H pseudo first order model for the initial rates of degradation proposes following the linear variation between $1/k_{obs}$ versus $[RR-84]_0$

according to eq. (1). In the Figure 9 can be seen the linearization of this relationship.

The value of the reaction rate constant on the catalyst surface (k) calculated using the slope in the L-H pseudo first order model was $1.09 \pm 0.31 \text{ mg}^* \text{L}^{-1} * \text{min}^{-1}$ and the L-H adsorption equilibrium constant (K_{L-H}) obtained with the intercept of straight line with y axis was $0.03 \pm 0.02 \text{ L}^* \text{mg}^{-1}$.

In the other L-H model represented by the eq. (2), considering that the H_2O_2 initial concentration, ψ and Si are constant for all experiments and only the RR-84 initial concentration is varied in the range of 20-100 $\text{mg}^* \text{L}^{-1}$, this last equation is transformed to the next form:

$$r_o = \frac{kK_{L-H}[RR-84]_o}{[1+K_{L-H}[RR-84]_o]} \quad (7)$$

This eq. (7) describes the information of how change the initial reaction rate with respect to RR-84 initial concentration, and considers the resistance due to the competitive adsorption of RR-84 in the catalytic active sites. The reaction initial rates are evaluated with the slope on the concentration curves (in the first 20 minutes of reaction) as a function of time for the discoloration reaction how is depict in the inset of the Figure 10 and with the initial rates values calculated in this inset was constructed the graph "L-H model" in this same Figure 10. Through the linear transformation of L-H model in the eq. (7) can be evaluated the corresponding reaction kinetic constant on the catalytic surface (k) and the L-H equilibrium constant (K_{L-H}) following the next equation:

$$\frac{[RR-84]_o}{r_o} = \frac{1}{K_{L-H}k} + \frac{[RR-84]_o}{k} \quad (8)$$

Once again, the k ($1.123 \pm 0.31 \text{ mg}^* \text{L}^{-1} * \text{min}^{-1}$) value is obtained with the slope and the K_{L-H} ($0.033 \pm 0.02 \text{ L}^* \text{mg}^{-1}$) equilibrium constant with the interception at the "y" axis in the linearization model and are shown in the Figure 11. These results are in accordance with the L-H pseudo first order model correlation (eq. (1) testing the reproducibility of calculation. However, in spite of the k and K_{L-H} constants in the L-H pseudo first order model obtain with eq. (1) are similar with the L-H model proposed in the eq. (8), the reaction kinetic $r_o = k_{obs}[RR-84]_o$ can only be validated at low initial concentrations ($<20 \text{ mg}^* \text{L}^{-1}$). Therefore, the L-H model is more suitable for these calculations.

Equilibrium dark adsorption

In order to verify the dual behavior of Fe_2O_3 NPs acting as photocatalyst or as Lewis acid catalyst, adsorption measurements were performed under darkness conditions varying the initial concentration of RR-84. Another method of L-H model take into account the pollutant adsorbed quantity (Q in $\text{mg}^* \text{g}^{-1}$) on catalyst surface in aqueous suspension:

$$Q = \frac{V * \Delta C}{m} \quad (9)$$

Where ΔC is the difference between initial (C_o) and equilibrium C_{eq} concentration of dye, V is the reaction volume in liters (0.1 L) and m is the mass of catalyst (Fe_2O_3) represented in grams of iron (0.00055 g), assuming in this particular case that all Fe present in the reaction mixture is converted into Fe_2O_3 NPs. However, we cannot reject the possibility of finding iron ions remaining in the reaction mixture.

The Figure 12 shows the RR-84 adsorption isotherm under darkness conditions on catalyst (Fe_2O_3) surface in the initial concentration range of 20-100 $\text{mg}^* \text{L}^{-1}$.

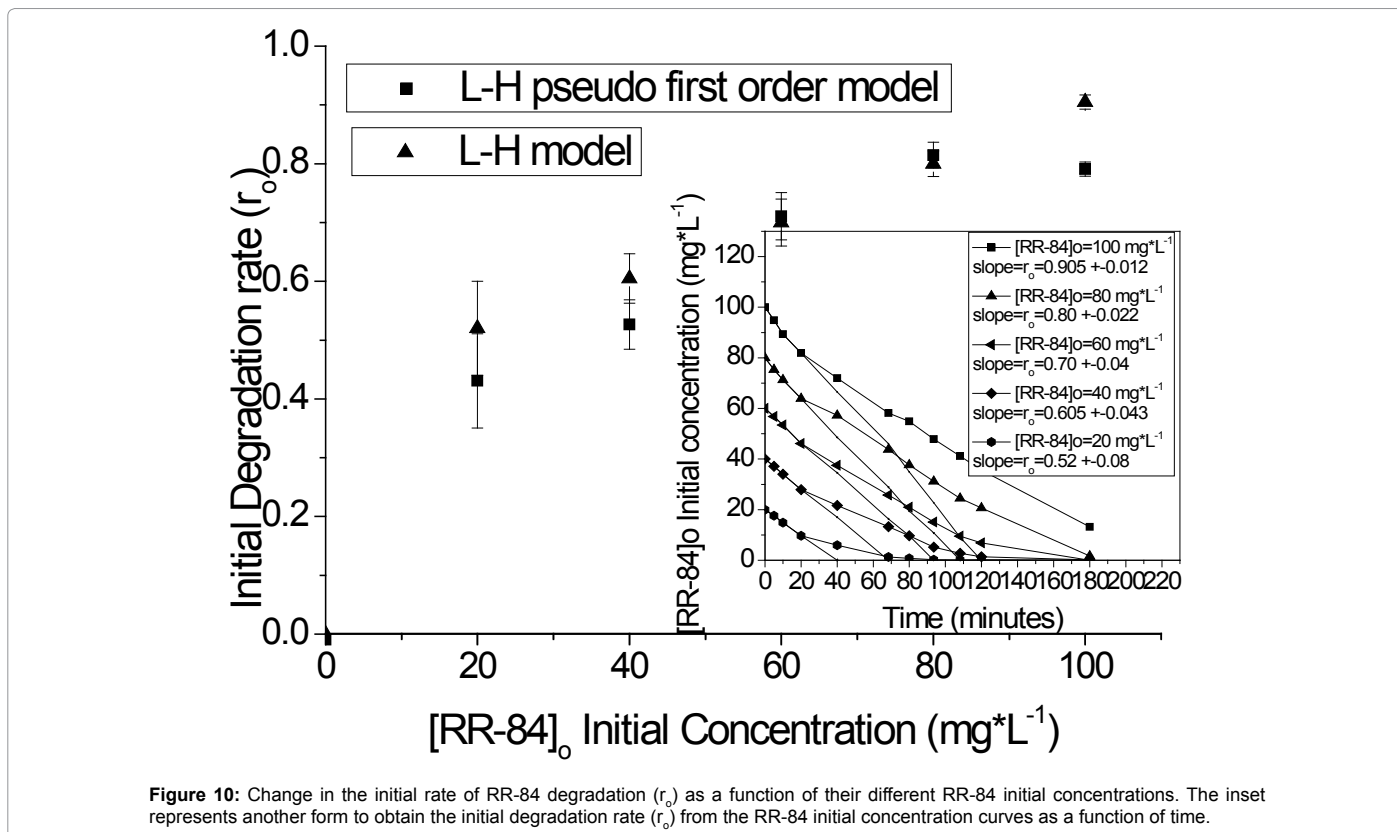


Figure 10: Change in the initial rate of RR-84 degradation (r_o) as a function of their different RR-84 initial concentrations. The inset represents another form to obtain the initial degradation rate (r_o) from the RR-84 initial concentration curves as a function of time.

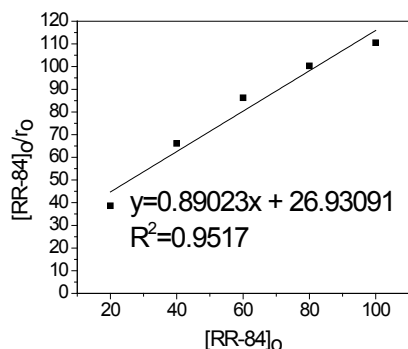


Figure 11: Variation of $[RR-84]_0/r_0$ as a function of initial concentration of RR-84.

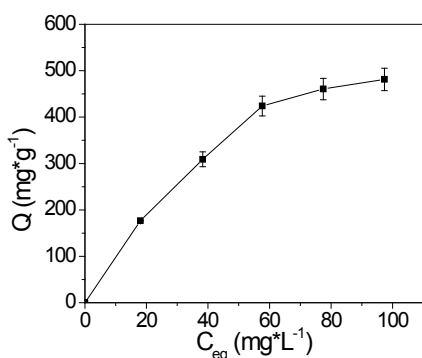


Figure 12: Adsorption isotherm of RR-84 on Fe_2O_3 , adsorbed amount of dye as a function of RR-84 equilibrium concentration.

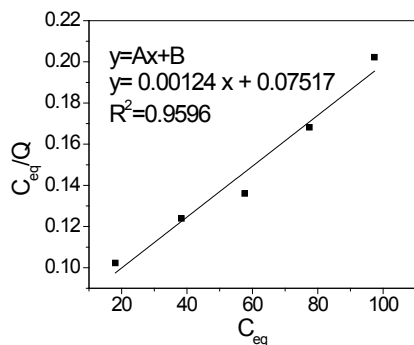


Figure 13: Obtainment of Langmuir monolayer adsorption constant for RR-84 adsorption on Fe_2O_3 under darkness conditions.

The amount of RR-84 adsorbed (Q) on the Fe_2O_3 NPs taking into account the coverage of the monolayer on the catalyst surface and can be followed by means of a Langmuir adsorption model in a low concentration range:

$$Q = \frac{Q_{\max} K_{\text{ads}} C_{\text{eq}}}{(1 + K_{\text{ads}} C_{\text{eq}})} \quad (10)$$

Where Q_{\max} is the maximum amount of dye adsorbed, K_{ads} is the equilibrium constant for adsorption and C_{eq} is the equilibrium concentration. Rearranging terms and linearizing the equation, forms the next expression:

$$\frac{C_{\text{eq}}}{Q} = \frac{1}{Q_{\max} K_{\text{ads}}} + \frac{C_{\text{eq}}}{Q_{\max}} \quad (11)$$

The Figure 13 shows a Graphic of C_{eq}/Q as a function of RR-84 equilibrium concentration (C_{eq}). The mass of catalyst selected for this analysis was 0.00055 g in terms of iron mass and represents the same iron concentration used in all experiments. It should be noted that there is no change in K_{ads} if the mass of catalyst is varied in this model. This variation in the catalyst mass only affect to Q_{\max} values.

The Langmuir adsorption constant (k_{ads}) was $0.016 \pm 0.004 \text{ L} \cdot \text{mg}^{-1}$ and the maximum amount of dye adsorbed (Q_{\max}) was $806.45 \text{ mg} \cdot \text{g}_{\text{catalyst}}^{-1}$. This high value of Q_{\max} could be explained due to the small size of Fe_2O_3 NPs and to the big amount of active sites present. Besides, if we could add 1 g of catalyst, this value could predict a high activity in azo dyes photodegradation as soon as the Fe_2O_3 phase that is interacting as photocatalyst is discovered. Unfortunately, we cannot use a catalyst load greater to 60 mg with respect to the elimination of $100 \text{ mg} \cdot \text{L}^{-1}$ of dye concentration, due to the limit on activity that the catalyst present. By this reason, it is better present the value of Q_{\max} with respect to the milligrams of catalyst used ($Q_{\max} = 0.80 \pm 0.18 \text{ mg} \cdot \text{mg}_{\text{catalyst}}^{-1}$). Indeed, this value also represents a high activity for the photodegradation of this azo dye even employing minimal quantities of catalyst.

In this work, the adsorption constants using Langmuir kinetic models resulted close, even conducting the adsorption measurements in darkness ($K_{\text{ads}} = 0.54 K_{\text{L-H}}$). The adsorption constant value under darkness condition could be lower than L-H equilibrium constants due to the inactivation of some catalytic active sites by the absence of illumination, affecting the adsorption processes in their surfaces. However, until here, we cannot reject the possibility of finding free iron ions or iron aqueous complexes in the mixture reaction that decrease the Fe_2O_3 NPs production efficiency, and by consequence, the adsorption process can be affected. However, this ratio between constants evidence that employing an iron concentration of $5.58 \text{ mg} \cdot \text{L}^{-1}$ with respect to the iron precursor salt $FeSO_4$ interacting with $1200 \text{ mg} \cdot \text{L}^{-1}$ of H_2O_2 at pH 3, it is possible the formation of Fe_2O_3 NPs acting as a catalyst to degrade $100 \text{ mg} \cdot \text{L}^{-1}$ of RR-84. The presence of these Fe_2O_3 NPs can stimulate adsorption systems that were fitted satisfactorily to the heterogeneous models of Langmuir-Hinshelwood.

Conclusions

$100 \text{ mg} \cdot \text{L}^{-1}$ of RR-84 azodye dissolved in 2.5 L of water can be completely discolored and partially degraded (up to 40%) in three hours, inside of a glass annular photoreactor, using Fe_2O_3 NPs prepared with the interaction of $FeSO_4/H_2O_2$ in aqueous suspensions at pH 3 and employing visible radiation.

The increasing on the iron amount in the reaction mixture leads to an improvement in photocatalytic activity and to a reduction of photodegradation time, however there is a limit of iron for each dye concentration. The increasing on the H_2O_2 concentration, also, presents a light enhanced in the photodegradation rate, but does not exceed the iron participation.

The dependence of the iron concentration on the initial discoloration rate (r_0) of RR-84 follows a similar relationship to ($r_0 \propto [Fe]^{0.78 \pm 0.06}$) using iron amounts less than 0.06 g.

Kinetic studies varying the RR-84 initial concentration and employing L-H model under illumination conditions proved adjust suitably with equilibrium dark adsorption measurements. The reaction

rate constant on surface of catalyst and the L-H equilibrium adsorption constant were $k=1.123 \pm 0.31 \text{ mg} \cdot \text{L}^{-1} \cdot \text{min}^{-1}$ and $KL-H=0.033 \pm 0.02 \text{ L} \cdot \text{mg}^{-1}$, respectively. Langmuir adsorption constant was $k_{ads}=0.016 \pm 0.004 \text{ L} \cdot \text{mg}^{-1}$ and the maximum amount of dye adsorbed was $Q_{max}=0.80 \pm 0.18 \text{ mg/mg}_{\text{catalyst}}^{-1}$. In spite of this Q_{max} is related to catalyst milligrams, the adsorption is high due probably to the large number of Fe_2O_3 NPs presents that represent more catalytic active sites due to their small size, predicting big photodegradation rates of organic pollutants.

The RR-84 photocatalytic degradation using Fe_2O_3 NPs is adjusted to L-H model of dye adsorption in a solid catalyst allowing think that Fenton's reaction $\text{FeSO}_4/\text{H}_2\text{O}_2/\text{H}_2\text{O}$ stimulates the formation of a Fe_2O_3 heterogeneous catalyst.

Acknowledgements

The authors acknowledge DGAPA-UNAM for financial support concerning the project IT101012 and funding given by the projects of CONACYT 167485 and 123122. The authors thank the technical support of P. AltuzarCoello, R. Moran, J. Campos and Ma. L. Ramón García for technical assistance. Authors also thank V. Garibay-Febles (IMP) for HRTEM analyses and C. F. Cano-Guzmán thanks to DGAPA-UNAM for the postdoctoral stipendium.

References

1. Boardman GR, Michelsen GD (1994) Fate of azo dyes in sludge. *Wat Res* 28: 1367-1376.
2. Mantzavinos D, Psillakis E (2004) Enhancement of biodegradability of industrial wastewaters by chemical oxidation pre-treatment. *J Chem Technol Biotechnol* 79: 431-454.
3. Prato-García D, Buitrón G (2011) Degradation of azo dye mixtures through sequential hybrid systems: Evaluation of three advanced oxidation processes for the pre-treatment stage. *J Photochem Photobiol A: Chem* 223: 103-110.
4. Walling C (1975) Fenton's reagent revisited. *J Acc Chem Res* 8: 125-131.
5. Neyens E, Baeyens J (2003) A review of classic Fenton's peroxidation as an advanced oxidation technique. *J Hazard Mater* 98: 33-50.
6. Fenton HJH (1894) Oxidation of tartaric acid in presence of iron. *J Chem Soc* 65: 899-910.
7. Haber F, Weiss J (1934) The catalytic decomposition of hydrogen peroxide by iron salts. *The Royal Society of LondonA: Math Phys Sci* 147: 332-351.
8. Merz JH, Waters WA (1949) The oxidation of aromatic compounds by means of the free hydroxyl radical. *J Chem Soc S* 15: 2427-2433.
9. Parra SR, Hernández I, Montiel E, Pérez JP, Sampieri A, et al. (2011) Photodegradation of phenol, 2-chlorophenol and o-cresol by iron oxide nanoparticles. *Nanosci Nanotech-Asia* 1: 31-40.
10. Vasanth K, Porkodi K, Selvaganapathi A (2007) Constrains in solving Langmuir-Hinshelwood kinetic expression for the photocatalytic degradation of Auramine O aqueous solution by ZnO catalyst. *Dyes Pigments* 75: 246-249.
11. Krishnakumar B, Swaminathan M (2011) Influence of operational parameters on photocatalytic degradation of a genotoxic azo dye Acid Violet 7 in aqueous ZnO suspensions. *Spectrochim Acta A: Mol Biomol Spectrosc* 81: 739-744.
12. Khezrianjoo S, Revanasiddappa HD (2012) Langmuir-Hinshelwood kinetic expression for the photocatalytic degradation of Metanil Yellow Aqueous solutions by ZnO catalyst. *Chem Sci J* 85: 1-7.
13. Ohtani B (2008) Preparing articles on photocatalysis—Beyond the illusions, misconceptions and speculation. *Chem Letters* 37: 217-229.
14. Sauer T, Cesconeto NG, José HJ, Moreira RFP (2002) Kinetics of photocatalytic degradation of reactive dyes in a TiO_2 slurry reactor. *J Photochem Photobiol A: Chem* 149: 147-154.
15. Poullos I, Tsachpinis I (1999) Photodegradation of textile dye Reactive Black 5 in the presence of semiconducting oxides. *J Chem Technol Biotechnol* 71: 349-357.
16. Silva CG, Faria JL (2003) Photochemical and photocatalytic degradation of an azo dye in aqueous solution by UV irradiation. *J Photochem Photobiol A: Chem* 155: 133-143.
17. Hachem C, Bocquillon F, Zahraa O, Bouchy M (2001) Decolourization of textile industry wastewater by the photocatalytic degradation process. *Dyes pigments* 49: 117-125.
18. Pare B, Jonnalagadda SB, Tomar H, Singh P, Bhagwat VW (2008) ZnO assisted photocatalytic degradation of acridine orange in aqueous solution using visible irradiation. *Desalin* 232: 80-90.
19. Galindo C, Jacques P, Kalt A (2001) Photooxidation of the phenylazonaphthol AO20 on TiO_2 : kinetic and mechanistic investigation. *Chemosphere* 45: 997-1005.
20. Parra S, Olivero J, Pulgarin C (2002) Relationships between physicochemical properties and photoreactivity of four biorecalcitrantphenylurea herbicides in aqueous TiO_2 suspensions. *Appl Catal B: Environ* 36: 75-85.